Int. J. Electrochem. Sci., 7 **(2012)** 12796 - 12807

International Journal of
ELECTROCHEMICAL
SCIENCE
www.electrochemsci.org

Poly(Diphenylamine) with Multi-walled Carbon Nanotube Composite Film Modified Electrode for the Determination of Phenol

Cheng-Yu Yang, Shen-Ming Chen[*]*, Tsung-Hsuan Tsai, Binesh Unnikrishnan*

Electroanalysis and Bioelectrochemistry Lab, Department of Chemical Engineering and Biotechnology, National Taipei University of Technology, No.1, Section 3, Chung-Hsiao East Road, Taipei 106, Taiwan (ROC).
[*]E-mail: smchen78@ms15.hinet.net

Received: 19 October 2012 / *Accepted:* 12 November 2012 / *Published:* 1 December 2012

In this study I report the electrochemical oxidation of phenol at a poly diphenylamine (PDPA)- multi-walled carbon nanotube (MWCNT) composite film modified glassy carbon electrode (GCE). PDPA was polymerized on the MWCNT modified GCE by cyclic voltammetry (CV) in 0.1 M H_2SO_4. The surface morphology of PDPA-MWCNT was studied using scanning electron microscope (SEM). The interfacial electron transfer phenomenon at the modified electrode was studied using electrochemical impedance spectroscopy (EIS). The PDPA-MWCNT composite film showed good electrocatalytic behavior towards the oxidation of phenol in pH 7. Phenol showed a well defined anodic peak at 0.65 V (vs. Ag/AgCl electrode). The MWCNT in PDPA-MWCNT film enhanced the anodic peak current by 8.48 and 2.36 times than that of MWCNT/GCE and PDPA/GCE electrode. The peak current increased linearly with phenol concentration. The amperometric determination of phenol at the composite film modified electrode showed linear range from 9.8 to 80 μM. This result shows that the proposed composite electrode may be developed for potential application in real sample analysis.

Keywords: poly diphenylamine, multi-walled carbon nanotube, phenol, cyclic voltammetry, amperometry

1. INTRODUCTION

Carbon materials have attracted a great deal of interests for both scientific fundamentals and potential applications in various new optoelectronic devices [1], such as graphite [2], carbon black [3], mesoporous carbon [4], carbon nanotube (CNT) [5–8], and graphene [9–12]. Among a wide variety of nanomaterials, CNTs have sparkled tremendous interests for sensor application due to their unique properties [13–17]. CNTs have been proved to be suitable material as electrodes or electrocatalyst

supports due to their many advantages such as high electronic conductivity for the promotion of electron transfer reactions and better electrochemical and chemical stabilities in aqueous and non-aqueous solutions [18]. Recently, electro-polymerization a conducting polymer film on the CNTs to attach them on the electrode surface are another interesting method [8, 19–21], but similar to casting with binder, the polymer film usually tends to grow into a bulk material, in which the CNTs are embedded in the polymer and do not contribute to the sequential protein attachment [22]. Composite materials based on the combination of CNT and conducting polymers have shown properties of the individual components with a synergistic effect [23–25].

Conducting polymers have become an important research focus during the past 30 years because of their unique optical, electronic, and mechanical properties with many potential applications [26–30]. Polymer film-coated electrodes can be differentiated from other modification methods because of their adsorption and covalent bonding, in that they usually involve multilayers, as opposed to the monolayers that are frequently encountered with the latter methods. Conductive/electroactive polymers, such as polypyrrole, polyaniline (PANI), polythiophene, etc. [31–36], are prepared through an electropolymerization procedure and used as modifiers for the construction of chemically modified electrodes [37–39]. Among various conducting polymers, poly (diphenylamine) (PDPA) is found to show many properties that are not comparable with other N-substituted PANI's, which include electrochemistry, conductivity, and electrochromic behavior [40–46]. These differences in properties between PANI and PDPA originate from the distinct changes in the backbone structures which are generated during polymerization. The mechanism for the polymerization of diphenylamine (DPA) has been reported to be different from other N-substituted anilines and aniline [46].

The present study is concerned with PDPA-MWCNT film effect on electrode behavior and the anticipation of electrostatic interaction between PDPA and the pretreated MWCNT with carboxylation hybrid film. The surface morphology of PDPA, MWCNT and PDPA-MWCNT film modified GCE has been examined by using SEM. The interfacial electron transfer phenomenon at the modified electrode was studied using electrochemical impedance spectroscopy (EIS). The cyclic voltammetric and amperometric techniques were used to study the mechanism of phenol oxidation.

2. EXPERIMENTAL

2.1 Apparatus

The cyclic voltammetric experiments were conducted on CHI 410A electrochemical workstation. A conventional three electrode system was used for cyclic voltammetry (CV) with GCE modified with MWCNT, PDPA and PDPA-MWCNT as working electrodes, a thin Pt wire as counter electrode and Ag/AgCl (sat. KCl) as reference electrode. EIS measurements were performed using IM6ex ZAHNER (Kroanch, Germany). SEM was performed using a Hitachi S-3000 H Scanning Electron Microscope. The amperometric experiments were performed using CHI 750 potentiostat with analytical rotator AFMSRX (PINE Instruments, USA).

2.2 Reagents and materials

MWCNTs with O.D. 10 – 15 nm, I.D. 2–6 nm, length 0.1–10 μm was obtained from Sigma–Aldrich. Diphenylamine (99 +%, A.C.S. reagent) was obtained from Aldrich, USA. 0.1 M phosphate buffer solution (PBS) was prepared from 0.1 M Na_2PO_4 and NaH_2PO_4 in doubly distilled deionized water to get a pH of 7. Inert atmosphere was set by passing N_2 over the solution during experiment.

2.3 Preparation of PDPA-MWCNT composite modified electrode

As purchased MWCNT was hydrophobic in nature and could not produce a stable and homogeneous dispersion in aqueous media. MWCNT was pretreated and functionalized by following the procedures reported earlier [47, 48]. 150 mg of MWCNT was heated at 350ºC for 2 h and cooled to room temperature. Then it was ultrasonicated for 4 h in concentrated HCl to remove impurities like amorphous carbon and metal catalysts. It was filtered and washed thoroughly with deionized water until the pH of the washing was 7. The filtered MWCNT was dried at 100ºC. Carboxylation of the MWCNT was done by sonicating the pretreated MWCNT in a mixture of sulfuric acid and nitric acid in 3:1 ratio for 6 h. It was then washed several times with deionized water until the washing was neutral.

GCE was polished using 0.05 μm alumina slurry and Buehler polishing cloth. To fabricate the PDPA-MWCNT modified electrodes, 1 mg of the functionalized MWCNT was dispersed into 1mL of doubly distilled deionized water by ultrasonication for 30 minutes. A well dispersed homogeneous solution of MWCNT was obtained. 4 μL of MWCNT dispersion was drop casted onto the well polished GCE and dried. Electropolymerization of DPA was done on MWCNT-GCE by continuous cycling in a three electrode system by cyclic voltammetry.

3. RESULTS AND DISCUSSIONS

3.1 Electropolymerization of DPA

Fig. 1 shows the cyclic voltammogram of the electropolymerization of DPA on MWCNT-GCE. CV was recorded by continuous potential cycling for 20 cycles in the range of –0.1 to 1.0 V vs. $Ag/AgCl_{sat}$ at a scan rate of 0.1 V s^{-1} in 5 M H_2SO_4 containing 1 x 10^{-3} M monomer concentration. The continuous growth of PDPA exhibits two redox processes. The first oxidation peak appears at 0.59 V and the second one appears at 0.76 V during the anodic scan. The oxidation peak at 0.59 V is due to the removal of one electron from the amino group to form a positively charged N, N′-diphenylbenzidine type ion radical (DPA^{+}•) [49]. Then, a removal proton from two such monomer radicals dimerizes to form a dimer of DPA. The coupling takes place at the para position, as shown in scheme 1[50]. Further oxidation leads to the growth of PDPA chain. During negative scan, the polymer is reduced by the protonation of the nitrogen atom in the backbone of the polymer. The reduction peaks appear at 0.42 V and 0.63 V during the cathodic scan. The anodic and cathodic peak

currents increase with the number of cycles indicating the deposition of the conducting material on the electrode surface.

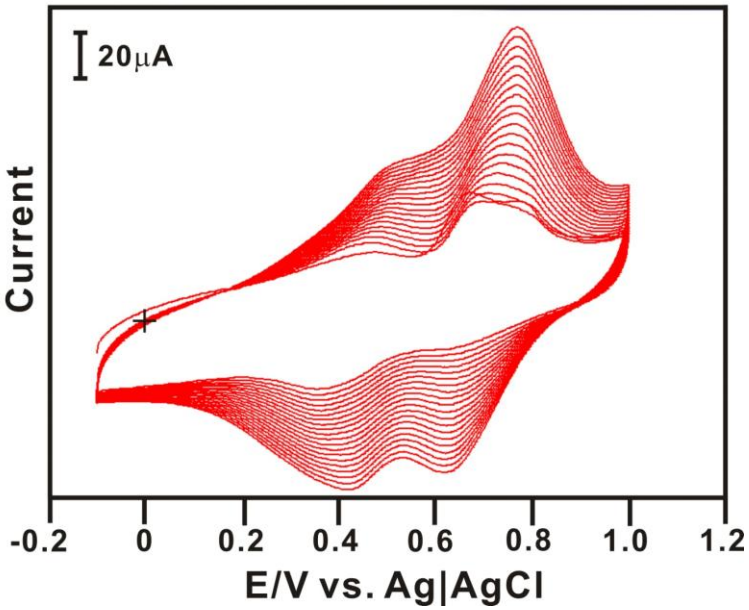

Figure 1. Electropolymerization of DPA on MWCNT/GCE for 20 cycles in 0.1 M H_2SO_4 containing monomer concentration 1x 10^{-3} M in the potential range of –0.1 to 1.0 V. Scan rate: 0.1V s^{-1}.

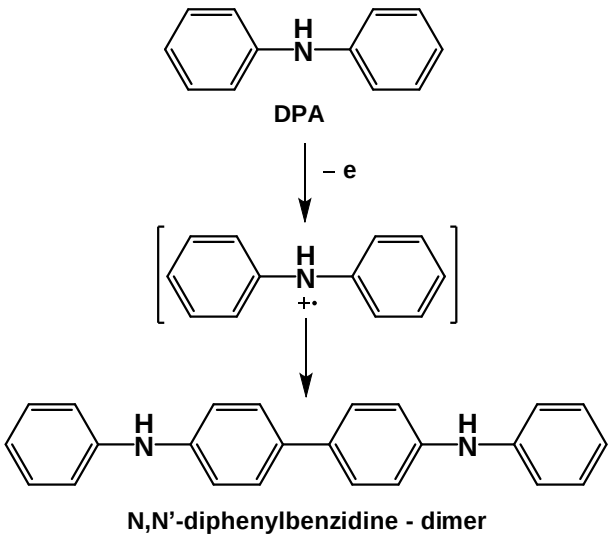

Scheme 1. Formation of N, N´-diphenylbenzidine type ion radical (DPA^{+}•) and dimer.

3.2 Surface morphological study of films by SEM

Fig. 2 shows the SEM images of various films deposited on ITO with same experimental conditions as mentioned above for GCE. It is clear that the three films have different m morphologies. MWCNT is distributed over the ITO during the drop casting process (fig. 2 (a)). FiG.2 (b) shows the

PDPA polymer distributed over the ITO surface. However, it is can be seen that the PDPA is not a uniform film. Lot of cavity like structure can been.

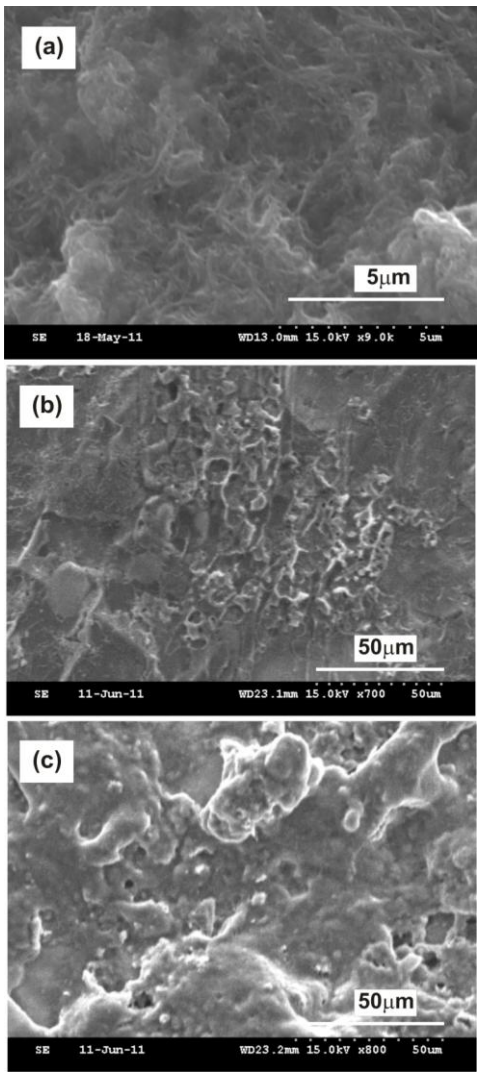

Figure 2. SEM images of (a) MWCNT, (b) PDPA, and (c) PDPA-MWCNT films.

It is reported earlier that continuous film of PDPA cannot be prepared by cyclic voltammetry [51]. This could be due to the solubility of the oligomers from the electrode surface. SEM image of PDPA-MWCNT composite film on ITO surface is shown in fig. 2 (c). The nature of interaction between MWCNT and PDPA is electrostatic. The oxidized form of PDPA is positive charged [52]. This helps PDPA globules adhere to the MWCNT forming a stable porous film.

3.3 Different scan rate studies of PDPA-MWCNT in pH7

The different scan rate studies were conducted for PDPA-MWCNT/GCE using CV in 0.1 M PBS pH 7 in the potential range of -1.0 to 1.0 V. Purified N_2 gas was purged into the buffer solution

for 10 minutes before recording the CV responses. The CV responses of PDPA-MWCNT/GCE at different scan rates are shown in fig.3. Both I_{pc} and I_{pa} increase linearly with the scan rate. The linear dependence of I_{pc} and I_{pa} with the scan rate is given in the inset of fig.3.

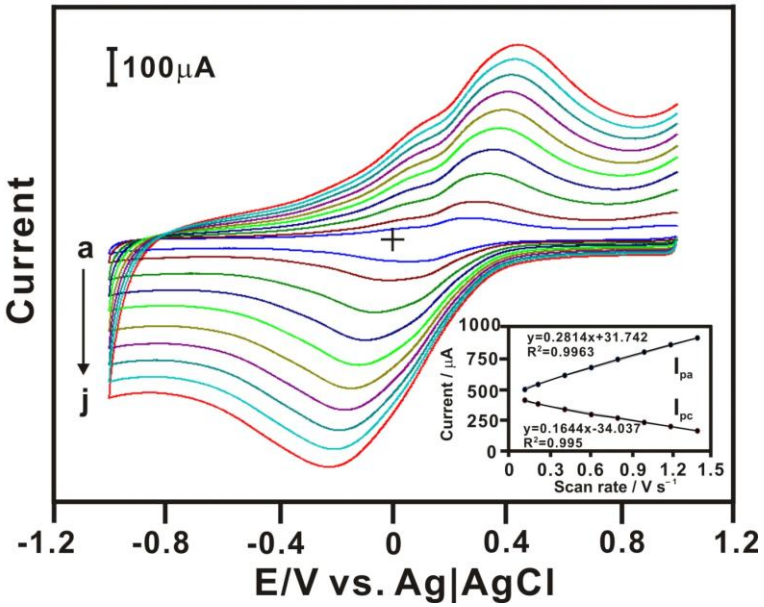

Figure 3. CVs recorded at PDPA-MWCNT/GCE in N_2 saturated 0.1 M PBS pH 7 at different scan rates from inner to outer are (a) 100, (b) 200, (c) 400, (d) 600, (e) 800, (f) 1000, (g) 1200, (h) 1400, (i) 1600 and (j) 1800 mV s^{-1} in the potential range of -1.0 to 1.0 V. The inset shows the linear dependence of I_{pc} and I_{pa} on scan rates.

This result shows that PDPA-MWCNT composite has electroactive sites and shows the redox peaks in pH 7. The film exhibits good linear relationship between I_{pc} and I_{pa} in such a wide range of scan rate from (a) 100, (b) 200, (c) 400, (d) 600, (e) 800, (f) 1000, (g) 1200, (h) 1400, (i) 1600 and (j) 1800 mV s^{-1}. This indicates the good stability of the film in pH 7. The inset in fig. 3 shows the plot of the PDPA-MWCNT signal of the anodic and cathodic peak current vs. scan rate. The corresponding linear regression equations were I_{pa} (μA) = 0.281v (V/s) + 31.74, R^2 = 0.9963, and I_{pc} (μA) = 0.164v (V/s) – 34.04, R^2 = 0.995. It indicates that the electrochemical reaction of PDPA-MWCNT is a surface-controlled process.

3.4 Electrochemical behavior of phenol at various electrodes

The electrochemical oxidation of phenol at different electrodes has been recorded by cyclic voltammetry in the potential range of -0.2 to 0.9 V at a scan rate of 0.1 V s^{-1}. The oxidation and reduction peaks of PDPA-MWCNT/GCE are separated as +200 and +5 mV. In Fig. 4(A), curve (a) indicates the CV signals of PDPA-MWCNT/GCE, (b) MWCNT/GCE, (c) PDPA/GCE, and (a') bare GCE pH 7 PBS. When comparing magnitude of current in pH 7 PBS, the (a) PDPA-MWCNT/GCE was higher than (b) PDPA/GCE, (c) MWCNT/GCE and (a') bare GCE in 0.1 M pH 7 PBS. The $E^{0'}$

was 125 mV for (a) PDPA-MWCNT/GCE and 425 mV for (c) PDPA GCE in 0.1 M pH 7 PBS. In the same buffer solution, there was no obvious response at curve (b) MWCNT/GCE and (a') bare GCE. Figure 4(B) shows the determination of phenol at different film by CV. It has been observed that at (a') bare GCE does not show any response for phenol.

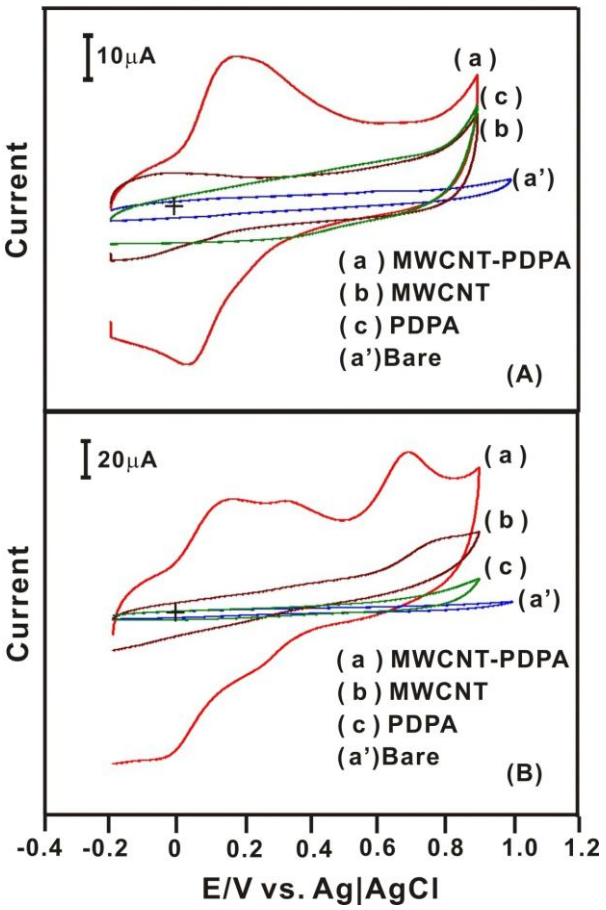

Figure 4. CVs of (a) PDPA-MWCNT/GCE, (b) MWCNT/GCE, (c) PDPA/GCE and (a') bare GCE in **(A)** pH 7 PBS and (B) pH 7 PBS containing 1.78 mM phenol at a scan rate of 0.1 V s^{-1}.

Phenol shows an oxidation peak at 814 mV and 750 mV at (b) MWCNT/GCE and (c) PDPA/GCE. At (a) PDPA-MWCNT/GCE, phenol shows the oxidation peak at around 650 mV. The shifts towards negative potential are 164 mV in comparison to (b) MWCNT/GCE and (c) PDPA/GCE. On comparison with the (b) MWCNT/GCE and (c) PDPA/GCE, the peak current is increased by 8.48 and 2.36 times. The increase in peak current and the shift in the oxidation peak potential show the good electrocatalytic behavior of PDPA-MWCNT/GCE electrode in comparison with the only (b) MWCNT/GCE, (c) PDPA/GCE and (a') bare GCE.

3.5 EIS studies of different films

Conducting polymers, electrolytes, surfactants, nanomaterials or semiconducting materials coated on the electrode surface change the double layer capacitance and interfacial electron transfer

resistance of the corresponding electrode. Impedance spectroscopy can reveal the interfacial changes due to the surface modification of electrodes [53]. Where R_s is the electrolyte resistance, R_{et} is charge transfer resistance, C_{dl} double layer capacitance and Z_w is Warburg impedance. The semicircle appeared in the Nyquist plot indicates the parallel combination of R_{et} and C_{dl} resulting from electrode impedance. The semicircles obtained at lower frequency represent a diffusion limited electron transfer process and those at higher frequency represent a charge transfer limited process, which were performed at the open circuit potential.

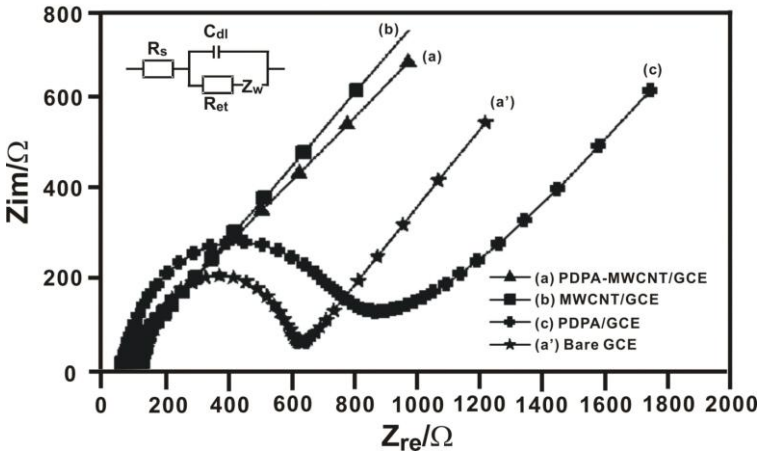

Figure 5. EIS of (a) PDPA-MWCNT (b) MWCNT, (c) PDPA modified GCE, and (a') bare GCE in 5 mM $Fe(CN)_6^{3-}/Fe(CN)_6^{4-}$ in pH 7 PBS. Applied AC voltage: open circuit potential, frequency: 0.1 Hz to 100 KHz.

The electrochemical impedance properties of (a) PDPA-MWCNT (b) MWCNT, (c) PDPA modified GCE, and (a') bare GCE are recorded in 5 mM $Fe(CN)_6^{3-}/Fe(CN)_6^{4-}$ in pH 7 PBS and represented as Nyquist plot (Z_{im} vs. Z_{re}) in fig.5. The inset of fig.5 shows the Randles equivalence circuit model used to fit the experimental data. From fig.5, (a') bare GCE and (c) PDPA/GCE exhibit a semicircle with 625 and 897 (Z'/Ω) at lower frequency region showing significant resistance towards the electron transfer process at the electrode surface. Whereas, MWCNT and PDPA-MWCNT modified GCE exhibit a very small semicircle region with 35 and 47 (Z'/Ω), which indicated very low impedance of the films. The low impedance of these two films are due to the high conducting nature of MWCNT and electrostatic interaction of negatively charged functionalized MWCNT and the positively charged PDPA.

3.6 Electrocatalytic oxidation of phenol at PDPA-MWCNT/GCE by CV and amperometric

The electrocatalytic property of the PDPA-MWCNT/GCE towards the oxidation of phenol was studied using CV. Fig.6 shows the CV obtained for electrocatalytic oxidation of phenol at PDPA-MWCNT/GCE in various concentrations (a to o). The anodic peak current linearly increases with increase in concentration of phenol from 3.96 μM to 177.8 mM. The linear depends on the I_{pa} versus concentration of phenol is given in inset of fig.6. The I_{pa} increases linearly with phenol concentration

with a slope of 0.202 μA μM^{-1} and the linear regression coefficient R^2 = 0.9905. The good linear response shows the promising electrocatalytic application of the proposed film in real sample analysis.

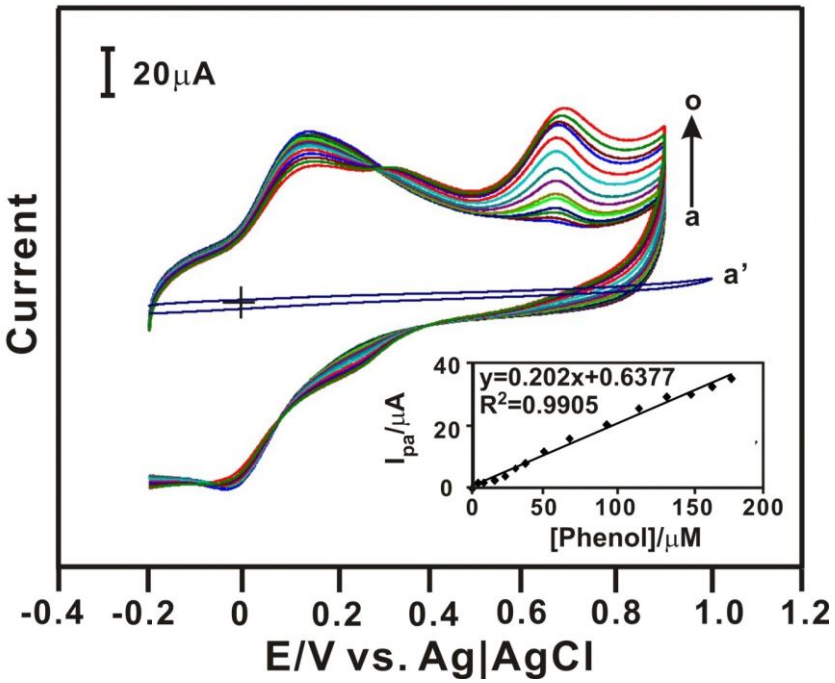

Figure 6. Cyclic voltammograms obtained for various concentrations of phenol were (a) 0, (b) 3.96, (c) 7.84, (d) 15.38, (e) 22.64, (f) 29.63, (g) 36.36, (h) 49.12, (i) 66.66, (j) 92.30, (k) 114.3, (l) 133.3, (m) 150.0, (n) 164.7, and (o) 177.8 μM at PDPA-MWCNT/GCE in N_2 saturated 0.1 M pH 7 PBS. The scan rate was 0.1 V s^{-1} in the potential range of -0.2 to 0.9 V. Inset shows the plot of anodic peak current (I_{pa}) vs. concentration of phenol.

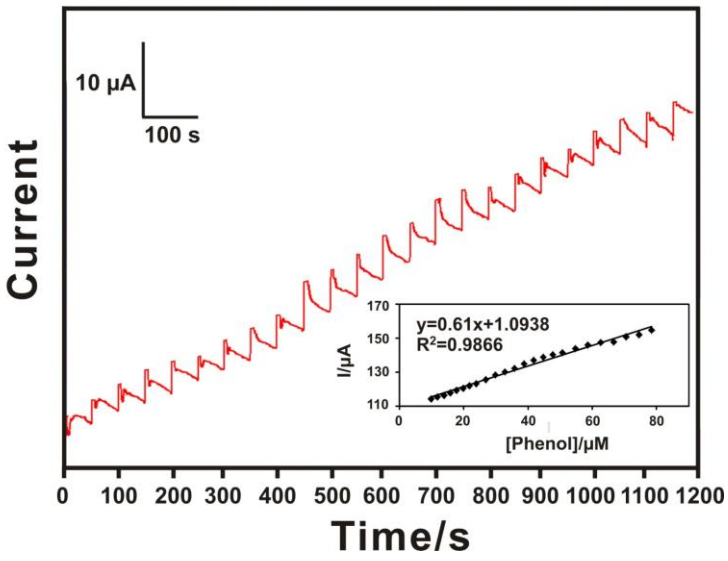

Figure 7. Amperometric i-t curve of phenol (9.8-80 □M) at PDPA-MWCNT/GCE modified rotating disc GCE in the applied potential of 0.65 V in N_2 saturated 0.1 M PBS solution pH 7. Rotation rate: 1200 RPM. The inset shows the plot of linear dependence of amperometric response on the on the concentration of phenol.

Table 1. Comparison of the determination of phenol by various electrochemical modified electrodes. Linear concentration range (LCR). Limit of Determination (LOD).

Modified electrode	Method	E_p(V)	Electrolyte	LCR (μM)	LOD (μM)	Sensitivity(A M^{-1} cm^{-2})	Ref.
Tyr-AuNPs/GCE	SWV	---	pH 7.0 PBS	0.1–1.1	0.07	6.92	[54]
Tyr-Au/CPE	Amperometric	-0.15	pH 7.0 PBS	0.4–480	0.006	12.3	[55]
silica sol–gel/Nafion/GCE	Amperometric	-0.2	pH 7.0 PBS	5.0–100	1.0	0.66	[56]
MWNT-Nafion-Tyr/GCE	Amperometric	-0.01	pH 7.0 PBS	1.0–19	0.13	4.29	[57]
CHT/laponite/PPO/GCE	Amperometric	-0.05	pH 6.5 PBS	0.011– 40	0.01	0.28	[58]
Tyr–Aucoll–graphite–Teflon	Amperometric	−0.10	pH 7.4 PBS	0.025–4	0.02	7.64	[59]
Tyr-TiO2 sol-gel/CE	Amperometric	0	pH 7.0 PBS	0.44–11	0.13	5	[60]
PDPA-MWCNT/GCE	Amperometric	0.65	pH 7.0 PBS	3.96–177.8	0.5	8.71	This work

RDE is a hydrodynamic electrochemical technique which involves the convective mass transport of reactants and products at the electrode surface, when the electrode is rotated at a specific speed [55]. The amperometric response of phenol at PDPA-MWCNT modified rotating disc GCE with a surface area of 0.07 cm^2 is shown in fig.7. The experiment was conducted at pH 7 PBS at an applied potential of 0.65 V with a rotation rate of 1200 RPM. Phenol solution in pH7 PBS was added at regular intervals of time. Electrocatalytic oxidation of phenol occurs at RDE in a totally mass transfer controlled condition, the limiting current increases linearly with the rotation rate. For every addition of phenol, a quick response (3 seconds) was observed and the oxidation current increases linearly. The inset shows the dependence of current on the concentration of phenol. The PDPA-MWCNT/GCE shows a good linear range of detection of phenol from 9.8 to 80 μM with a slope of 0.61 □A □M^{-1}. The correlation coefficient (R^2) was found to be 0.9866 and the sensitivity is 8.714 A M^{-1} cm^{-2}. The linear range and sensitivity observed with PDPA-MWCNT/GCE is in general comparable with most of the modified electrode reported in the literature [54–60] (Table 1). The higher linear concentration range (LCR) of PDPA-MWCNT modified electrode, may be the result of the PDPA film bound to the MWCNT film on electrode surface. Similarly, the PDPA-MWCNT/GCE modified electrode for the detection of phenol also has a higher sensitivity.

4. CONCLUSIONS

Fabrication of PDPA-MWCNT composite film modified GCE and its application for phenol determination reduction. DPA was successfully electropolymerized onto MWCNT modified GCE by cyclic voltammetry in 5 M H_2SO_4. The surface morphology of PDPA and PDPA-MWCNT films were characterized by SEM. The study shows PDPA is formed as non-continuous and porous type film on the electrode surface and not as a continuous smooth film. The MWCNT in the PDPA-MWCNT composite enhanced the anodic peak current of phenol 8.48 and 2.36 times than that of MWCNT/GCE and PDPA/GCE electrode. The amperometric determination studies showed that the composite film has quick response (3 seconds) and a good linear range of from 9.8 to 80 μM.

ACKNOWLEDGEMENTS
This work was supported by The National Science Council of Taiwan (ROC).

References

1. H. Zhu, J. Wei, K. Wang and D. Wu, *Sol. Energy Mater. Sol. Cells*, 93 (2009) 1461.
2. X. Hu, K. Huang, D. Fang and S. Liu, *Materials Science and Engineering B*, 176 (2011) 431.
3. Y. S. Park and H. K. Kim, *Current Applied Physics*, 11 (2011) 989.
4. E. Ramasamy and J. Lee, *Carbon*, 48 (2010) 3715.
5. J. Zhang, X. Li, W. Guo, T. Hreid, J. Hou, H. Su and Z. Yuan, *Electrochimica Acta*, 56 (2011) 3147.
6. C. T. Hsieh, B. H. Yang and J. Y. Lin, *Carbon*, 49 (2011) 3092.
7. M. Y. Yen, M. C. Hsiao, S. H. Liao, P. I Liu, H. M. Tsai, C. C. M. Ma, N. W. Pu and M. D. Ger, *Carbon*, 49 (2011) 3597.
8. K.C. Lin, T.H. Tsai and S.M. Chen, *Biosensors and Bioelectronics*, 26 (2010) 608.
9. W. Hong, Y. Xu, G. Lu, C. Li and G. Shi, *Electrochemistry Communications*, 10 (2008) 1555.
10. L. Wan, S. Wang, X. Wang, B. Dong, Z. Xu, X. Zhang, B. Yang, S. Peng, J. Wang and C. Xu, *Solid State Sciences*, 13 (2011) 468.
11. G. Zhu, T. Xu, T. Lv, L. Pan, Q. Zhao and Z. Sun, *Journal of Electroanalytical Chemistry*, 650 (2011) 248.
12. T.H. Tsai, S.C. Chiou and S.M. Chen, *Int. J. Electrochem. Sci*., 6 (2011) 3333.
13. H. Paloniemi, M. Lukkarinen, T. Aaritalo, S. Areva, J. Leiro, M. Heinonen, K. Haapakka and J. Lukkari, *Langmuir*, 22 (2006) 74.
14. Z.W. Pan, S.S. Xie, B.H. Chang, L.F. Sun, W.Y. Zhou and G. Wang, *Chem. Phys. Lett.*, 299 (1999) 97.
15. Z.F. Liu, Z.Y. Shen, T. Zhu, S.F. Hou, L.Z. Ying, Z.J. Shi and Z.N. Gu, *Langmuir*, 16 (2000) 3569.
16. Y.C. Choi, Y.M. Shin, D.J. Bae, S.C. Lim, Y.H. Lee and B.S. Lee, *Diam. Relat. Mater.*, 10 (2001) 1457.
17. B. Wu, J. Zhang, Z. Wei, S.M. Cai and Z.F. Liu, *J. Phys. Chem. B*, 105 (2001) 5075.
18. P. Santhosh, K.M. Manesh, A. Gopalan, K.P. Lee, *Sensors and Actuators B*, 125 (2007) 92.
19. J.H. Kim, Y.S. Lee, A.K. Sharma and C.G. Liu, *Electrochim. Acta*, 52 (2006) 1727.
20. C. Peng, S.W. Zhang, D. Jewell and G.Z. Chen, *Progr. Nat. Sci.*, 18 (2008) 777.
21. Y.L. Yao, K.K. Shiu, *Electrochim. Acta*, 53 (2007) 278.
22. Y. Hu, Z. Zhao and Q. Wan, *Bioelectrochemistry*, 81 (2011) 59.
23. K.M. Manesh, P. Santhosh, A.I. Gopalan, K.-P. Lee, *Electroanalysis*, 18 (2006) 1564.
24. P. Santhosh, K.M. Manesh, A.I. Gopalan, K.-P. Lee, *Electroanalysis*, 18 (2006) 894.
25. P. Santhosh, K.M. Manesh, A. Gopalan, K.-P. Lee, *Anal. Chim. Acta*, 575 (2006) 32.
26. T.H. Tsai, S.C. Chiou and S.M. Chen, *Int. J. Electrochem. Sci*., 6 (2011) 3938.
27. T.H. Tsai, T.W. Chen and S.M. Chen, *Electroanalysis*, 22 (2010) 1655.
28. T.H. Tsai, K.C. Lin and S.M. Chen, *Int. J. Electrochem. Sci*., 6 (2011) 2672.
29. T.H. Tsai, T.W. Chen, S.M. Chen and K.C. Lin, *Int. J. Electrochem. Sci*., 6 (2011) 2058.
30. T.W. Chen, T.H. Tsai, S.M. Chen and K.C. Lin, *Int. J. Electrochem. Sci*., 6 (2011) 2043.
31. T.H. Tsai, S.H. Wang, S.M. Chen, *Int. J. Electrochem. Sci*., 6 (2011) 1655.
32. R.W. Murry, A.G. Ewing, R.A. Durst, Anal. Chem. 59 (1987) 379A.
33. C. Mousty, B. Galland, S. Cosnier, Electroanalysis 13 (2001) 186.
34. M.H. Pournaghi-Azar, R. Ojani, J. Solid State Electrochem. 4 (2000) 75.
35. T.H. Tsai, Y.C. Huang, S.M. Chen, *Int. J. Electrochem. Sci*., 6 (2011) 3238.
36. T.H. Tsai, S.H. Wang, S.M. Chen, *J. Electroanal. Chem.*, 659 (2011) 69.
37. T.H. Tsai, T.W. Chen, S.M. Chen, *Int. J. Electrochem. Sci*., 6 (2011) 4628.

38. T.H. Tsai, Y.C. Huang, S.M. Chen, M.A. Ali, F.M.A. Alhemaid, *Int. J. Electrochem. Sci*., 6 (2011) 6456.
39. T.H. Tsai, T.W. Chen, S.M. Chen, R. Sarawathi, *Russ. J. Electrochem.*, 48 (2012) 291.
40. K. Feher, G. Inzlet, *Electrochim. Acta*, 47 (2002) 3551.
41. G. Inzelt, *J. Solid State Electrochem.*, 6 (2002) 265.
42. M.S. Wu, T.C. Wen and A. Gopalan, *Mater. Chem. Phys.*, 74 (2002) 58.
43. C.Y. Chung, T.C. Wen and A. Gopalan, *Electrochim. Acta*, 47 (2001) 423.
44. L.H. Guay, J. Dao and M. Leclerc, *Synth. Met*., 29 (1989) E383.
45. J. Guay, R. Paynter and L.H. Dao, Macromolecules, 23 (1990) 3598.
46. Y.T. Tsai, T.C. Wen and A. Gopalan, *Sensors and Actuators B*, 96 (2003) 646.
47. S. Jeykumari, D. R. Ramaprabhu and S. Narayanan, *Carbon*, 45 (2007)1340.
48. H. Su, R. Yuan, Y. Chai, Y. Zhuo, C. Hong, Z. Liu and X. Yang, *Electrochimica Acta*, 54 (2009) 4149.
49. A. Bhageri, M.R. Nateghi and A.M assoumi, *Synthetic Metals*, 97 (1998) 85.
50. N. Comisso, S. Daolio, G. Zotti, S. Zecchin, R. Salmaso, and G. Mengoli, *J. Electroanal. Chem.*, 255 (1988) 97.
51. D. Ragupathy, A.I. Gopalan and K.P. Lee, *Microchim Acta*, 166 (2009) 303.
52. E. Katz, I. Willner, Electroanalysis, 15 (2003) 913.
53. H.O. Finklea, D.A. Snider and J. Fedyk, *Langmuir*, 9 (1993) 3660.
54. B.C. Janegitz, R.A. Medeiros, R.C. Rocha-Filho, O. Fatibello-Filho, *Diamond & Related Materials*, 25 (2012) 128.
55. S. Liu, J. Yu, H. Ju, *J. Electroanal. Chem.*, 540 (2003) 61.
56. M. A. Kim, W.-Y. Lee, *Anal. Chim. Acta*, 479 (2003) 143.
57. Y.C. Tsai, C.C. Chiu, *Sensor Actuat.* B,125 (2007) 10.
58. Q. Fan, D. Shan, H. Xue, Y. He and S. Cosnier, *Biosens. Bioelectron*., 22 (2007) 816.
59. V. Carralero, M.L. Mena, A. Gonzalez-Cortes, P. Yanez-Sedeno and J.M. Pingarron, *Biosens. Bioelectron*., 22 (2006) 730.
60. J. Kochana, A. Gala, A. Parczewski, J. Adamski, Anal Bioanal Chem, 391 (2008) 1275.